



# Newcastle University ePrints

Benson S, AbuBakar A, Dow RS. [Progressive collapse analysis of a damaged box girder in longitudinal bending.](#)

*In: 12th International Symposium on Practical Design of Ships and Other Floating Structures. 2013, Gyeongnam Province, South Korea.*

**Copyright:** The definitive version of this article, published by PRADS, 2013.

**Date deposited:** 29<sup>th</sup> July 2014

**Version of file:** Author final



This work is licensed under a [Creative Commons Attribution-NonCommercial 3.0 Unported License](#)

ePrints – Newcastle University ePrints

<http://eprint.ncl.ac.uk>

# Progressive Collapse Analysis of a Damaged Box Girder in Longitudinal Bending

S Benson<sup>1)</sup>, A AbuBakar<sup>2)</sup> and RS Dow<sup>1)</sup>

<sup>1)</sup> School of Marine Science and Technology, Newcastle University, Newcastle upon Tyne, UK

<sup>2)</sup> Department of Maritime Technology, University Malaysia Terengganu, Terengganu, Malaysia

## Abstract

Estimating the residual ultimate strength of a severely damaged hull structure is important for determining recoverability, seaworthiness or assessing the capabilities of different structural configurations for withstanding damage. However, the estimation of ultimate strength, including a realistic representation of damage, is a complex problem and recourse must be made to advanced numerical methods. This paper provides a comparative assessment of several nonlinear finite element analysis approaches for the analysis of a small scale box girder structure in intact and damaged scenarios. Three severe damage scenarios are simulated, and the ultimate strength of the damaged girder is then calculated using several techniques. The results demonstrate the significance of the residual in plane stresses sustained during the onset of damage.

## Keywords

Ultimate strength; damage; nonlinear finite element analysis; progressive collapse

## Introduction

A critical strength measure of a thin plated box girder structure, such as the main hull of a ship, is the ability to withstand combinations of vertical and horizontal bending moments acting upon the longitudinally continuous structure. The maximum capacity of a hull girder under a pure longitudinal bending moment, often referred to as its ultimate strength, can be determined using several numerical approaches including nonlinear finite element analysis and simplified analytical methods. These approaches are generally referred to as progressive collapse analysis.

If a portion of the longitudinally effective structure is ruptured or severely damaged through collision, grounding or malicious attack, the ultimate capacity of the hull girder will inevitably be reduced. An assessment of residual ultimate strength in a damaged condition is thus useful for determining recoverability, seaworthiness or assessing the capabilities of a particular structural ar-

angement for withstanding damage.

This paper provides a comparative assessment of several nonlinear finite element analysis (NLFEM) approaches for the analysis of a small box girder structure in intact and damaged scenarios. The box girder replicates one of a series of structures originally tested by Gordo and Guedes Soares (2009). In this study the girder is first analysed when intact and then with ruptured penetrations simulated using a large indenter to represent damage. The results demonstrate the significance of the residual stresses sustained in the damage simulation.

## Background

Longitudinal progressive collapse involves nonlinear buckling and collapse of compressed portions of a box girder beam. Simplified approaches have been proposed to solve the progressive collapse problem, and several continue to be developed. They range in complexity and include simple closed form empirical formulae (Paik and Mansour, 1995), interframe progressive collapse methods (Smith, 1977) and compartment level methods (Benson et al., In press).

NLFEM is also a viable option for hull girder strength assessment. However, from a design perspective, NLFEM requires detailed knowledge of the geometry, imperfections and residual stresses in the structure. These are not necessarily well defined, even in structures physically tested in carefully controlled laboratory environments. Furthermore, from an analysis perspective, NLFEM requires considerable computer time both in setting up and solving the discrete model. Elements must be sized sufficiently small to represent the local structure adequately. The number of elements for an entire hull girder mesh can easily run to several hundred thousand, which becomes computationally expensive for NLFEM analyses.

Nethertheless, NLFEM is attractive when considering damage scenarios. The method is highly flexible. It can be used to model the damage scenario itself as well as the progressive collapse problem. Complex damage scenarios can be analysed provided sufficient information is known about the material properties, impact energy and boundary conditions. The finite element

model will retain geometric and material information from a damage simulation, for example the residual stresses in the remaining structure, and will propagate this information into a progressive collapse assessment.

An early application of NLFEM for the analysis of hull girders is presented by Kutt et al. (1985), who used a classification society NLFEM program (USAS) to calculate the longitudinal strength of four ship hulls including a passenger ship and a tanker. Results from nonlinear NLFEM analyses of box girders are presented by Qi et al. (2005). Analyses of tanker structures using large scale NLFEM models are made by Amlashi and Moan (2009).

The complexities of the ruptured zone after a collision or grounding are clearly shown from experimental work by numerous authors. For example, a series of full scale experiments by Wevers & Vredeveldt (1999) demonstrate the effects of a collision on different side shell scantlings. NLFEM simulations by AbuBakar & Dow (2013) present a series of large scale collision scenarios between two merchant ships. NLFEM studies demonstrating the severity and complexity of an actual ship collision have also been reported by Ehlers & Tabri (2012) amongst others.

These studies concentrate on the damage simulation itself, in particular the methods used to model the material behavior to capture high strain effects such as necking and fracture. Further work has been completed to capture the post damage residual strength of the hull girder. For example, Ehlers et al. (2013) considered the effect of the damage on the ultimate strength of the ship, although the ultimate strength calculations were limited to interframe progressive collapse calculations.

## Finite Element Methods

This paper provides a comparative assessment of several NLFEM approaches for the analysis of box girder structures in intact and damaged scenarios. Both static implicit and dynamic explicit solvers are used with the commercial software program ABAQUS. A summary of static and dynamic solvers are now given in relation to the box girder bending moment problem.

### *Static Implicit Methods*

Typically, NLFEM analyses of hull girder progressive collapse utilise a static solver together with an equilibrium convergence iterator using either the Riks arc length method or modified Newton-Raphson method. The static solver assumes that the time dependent mass and inertia effects are small and thus can be neglected. This assumption implies a quasi-static structural response, which is usually valid if the loading frequency is less than a quarter of the lowest natural frequency of the structure.

In the context of box girder analysis, the static solver is usually used in conjunction with an implicit convergence method. This means that equilibrium between external and internal forces at each increment is solved by carrying out further iterations until equilibrium is achieved within a specified tolerance. This allows rela-

tively large increment sizes to be used at the expense of requiring multiple iterations of each increment.

Several convergence methods are generally available. The Newton-Raphson method is particularly advantageous when the response nonlinearity is gradual, and will often result in an efficient and accurate solution time. The Riks method is employed when the response is more discontinuous, with sharp nonlinearities. Box girder collapse is typically characterised by a relatively sudden departure from a linear response as the imposed load approaches the ultimate strength, which is due to the compressed beam buckling. The Riks method was therefore used for all the implicit analyses conducted in this study.

### *Dynamic Explicit Methods*

The implicit static approach assumes that the box girder response can be characterised as quasi static. However, damage simulations such as are shown in this paper must be characterised as dynamic, thus including mass and damping effects. Use of a dynamic solver has been shown to be essential for ship collision, grounding and blast loading of ship structures where the damage is sustained relatively quickly. This paper compares the effectiveness of using a dynamic solver for the progressive collapse analysis in addition to its application in damage simulation.

In a dynamic NLFEM simulation mass-acceleration and damping-velocity terms need to be satisfied in the equilibrium equation, creating a time dependent simulation. The mass and time dependent loading or displacement of the NLFEM model must be adequately defined in the pre-processor. In the types of analysis covered in this paper, the inclusion of additional terms in the equilibrium equation adds a considerable time penalty to the solver, and the use of an implicit solver makes many analyses unfeasibly time consuming. Therefore, a more efficient approach is to use an explicit solver. This procedure does not ensure equilibrium of internal and external forces at the end of each increment. Instead, the stiffness matrix at the beginning of the increment (time  $t$ ) is used to predict the solution at the end of the increment (time  $t+\delta t$ ). This means the time step must be sufficiently small to prevent the residual between the calculated solution and the actual solution becoming too large. If the time increment is set too large the calculated response may drift too far from the actual solution to provide reliable results.

In addition to analysing the progressive collapse of a box girder, the dynamic-explicit solver approach is also suitable for analysing impact damage and rupture. Modelling of rupture requires a well-defined failure model specific to the material properties and element size. The failure model for the high tensile steel investigated in this study is detailed further in the next section. All damage simulations have been conducted using the general approach described by AbuBakar and Dow (2013).

## Material Properties

Appropriate definitions of material properties for high tensile steel grade (S690) are important to adequately characterise high strain and rupture in the damage simulations. The material properties are identical in all analyses and are now summarised.

### Stress Strain Relationship

The material characteristics, in the form of a true stress-strain curve, must be adequately represented in the finite element model to ensure an accurate treatment of plasticity. This is important for the progressive collapse analysis and also for realistically modelling rupture in the damage tests. Therefore a literature search was conducted to better define the nonlinear response for the material. The nominal yield strength of the high tensile steel S690 is 690MPa with a Young's modulus of 200GPa. No tensile test data for the steel used in the box girder experiments is available, although manufacturers quoted values are 732MPa at yield and 808MPa at 15% elongation. However, tests on specimens from 4mm plate by the same research team are reported as 680MPa at yield and 764MPa at 10.5% elongation (Gordo and Guedes Soares, 2011). A separate study presents a complete stress-strain curve for S690 (Sedlacek and Müller, 2001). This curve can be described using a modified power law, which was developed to accurately represent the initial yield plateau characteristic of steel (Alsos et al., 2008). The power law uses a step function as follows:

$$\sigma_{eq} = \begin{cases} \sigma_Y & \text{if } \varepsilon_{eq} \leq \varepsilon_{plat} \\ K(\varepsilon_{eq} - \varepsilon_0)^n & \text{otherwise} \end{cases} \quad (1)$$

$$\varepsilon_0 = \varepsilon_{plat} - \left(\frac{\sigma_Y}{K}\right)^{1/n} \quad (2)$$

The constants for S690 used in this study are based on the curve by Sedlacek and Muller as follows:  $K=1250\text{MPa}$ ,  $n=0.12$ ,  $\varepsilon_{plat}=0.0124$ ,  $\sigma_0=745\text{MPa}$  and  $E=211\text{GPa}$ . The stress-strain curve is shown in Fig. 1.

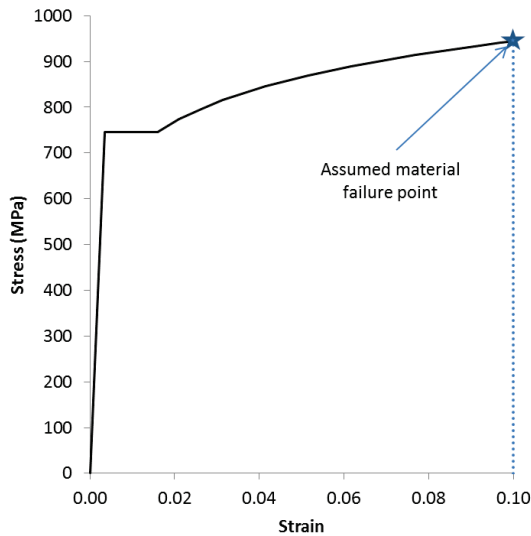


Fig. 1: S690 Stress-Strain Curve

## Failure Model

The material failure model is used in conjunction with the material properties described previously. The failure model permits the rupture of the box girder structure when the material exceeds the allowable or maximum strain in any direction during penetration of the indenter.

The material failure model is based on the forming limit diagram (FLD) method, which is a concept introduced by Keeler and Backofen (1964) to determine the amount of deformation that a material can withstand prior to the onset of necking instability. The maximum strains that sheet material can sustain prior to the onset of necking are referred to as the forming limit strains as described in the ABAQUS documentation.

Considering the forming limit strains as rate independent effects in the FLD method, details of which can be found in Jie et al. (2009), the following relationships are used:

$$\varepsilon_1 = \begin{cases} \frac{n}{(1+r_\varepsilon)} & \text{if } r_\varepsilon \leq 0 \\ \frac{3r_\varepsilon^2 + (2+r_\varepsilon)^2 n}{2(2+r_\varepsilon)(1+r_\varepsilon+r_\varepsilon^2)} & \text{if } r_\varepsilon > 0 \end{cases} \quad (3)$$

where  $r_\varepsilon = \varepsilon_2/\varepsilon_1$  is the strain ratio.  $r_\varepsilon=0$  for plane strain  $r_\varepsilon=-0.5$  for simple tension and  $r_\varepsilon=1$  biaxial tension, which is the basis for localized necking failure.  $n$  is the hardening constant.

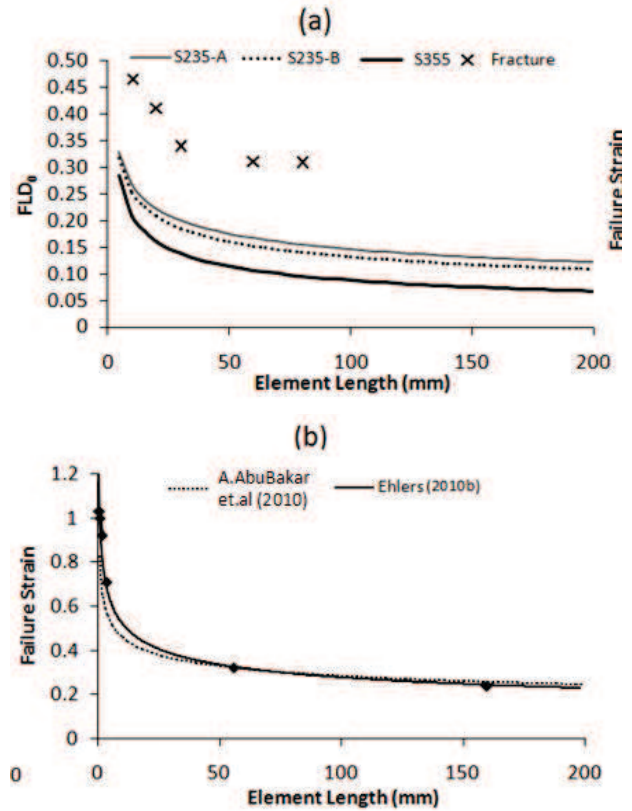


Fig. 2: (a) The scaling forming limit diagram at onset necking versus element length [32]. (b) The failure strain versus element length.

For all of the simulations carried out the friction coeffi-

cient was set at 0.3 and the displacement at failure considered to be  $\epsilon_u L$ . Where  $\epsilon_L$  is ultimate strain, approximately  $0.5\epsilon_f$  where  $\epsilon_f$  is fracture strain and  $L$  is characteristic element length. In the post necking regime the element characteristic size has a significant influence on the accuracy of the results. For shell and 2D elements,  $L$  is square root of the integration area and for 3D elements  $L$  is the cube root of the integration of volume.

The rupture of the structure depends upon  $FLD_0$ , which is the point of minimum strain under plane strain conditions when local necking occurs. For this study a rupture strain of 0.1 was assumed, as shown in Fig. 1. The  $FLD_0$  in relation to element length in Fig. 2a introduced by AbuBakar et al. (2010) are used throughout this analysis. Fig. 2b shows the relationship of rupture strain between AbuBakar et al. (2010) and Ehlers (2010), where the rupture point according to the element length is alike. Ehlers also shows that the thicknesses of the plate do not give any significant effect to the rupture strain point.

### Analysis of Intact Box Girder

This paper replicates experiments on a simple multi-frame box girder structure, which was originally physically tested at the Technical University of Lisbon (IST) using a four point bending rig. The girders were built simply; because it is a small scale model the stiffeners are placed on the outside of the shell to enable welding access during construction. The principal box girder dimensions are shown in Fig. 3 with spacing and thicknesses presented in Table 1.

Table 1 – Box Girder Properties

Specimen Length (mm)	Frame Spacing (mm)	Plate Thickness (mm)	Stiffener Height (mm)	Stiffener Thickness (mm)
1000	200	4	20	4

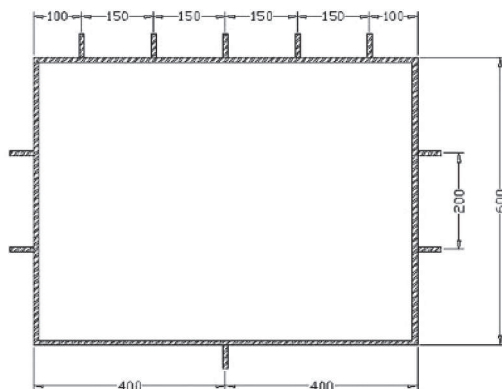


Fig. 3: Box girder cross section [source: [2]].

The length includes an additional 100mm span at each end, which was connected to the bending rig by a heavy bulkhead. Load was applied through hydraulic jacks connected to a strong box, which in turn rests on the

outer supports of the bending rig. All the supporting structure was constructed from thick high tensile steel. The test specimen was welded between the outer supports whilst the outer edges of the supports rested on the floor. The rig thus produces a four point bending load, with the central section under pure bending moment.

To ensure a robust modelling approach, the parameters which are used to replicate various important aspects of the experimental setup were first defined using preliminary analyses where appropriate. A summary of these preliminary tests are now presented.

### Model extents and boundary conditions

A common idealisation when analysing a hull section or box girder section is to only analyse a section or slice of the complete geometry. This reduces the size and complexity of the mesh, allowing efficient use of the NLFEM solver. It is especially important when simulating damage scenarios, which require very small increment sizes and may take a substantial amount of computation time to complete.

Therefore, a representation of the IST box girder test section as an isolated unit was first developed in Abaqus CAE. Bending moment is applied through rotation controls applied to one or both ends of the section. Suitable boundary conditions can be set to ensure the rotation produces a pure bending moment without introducing an eccentric longitudinal force. In this study, the section boundary conditions were set as shown in Fig. 4.

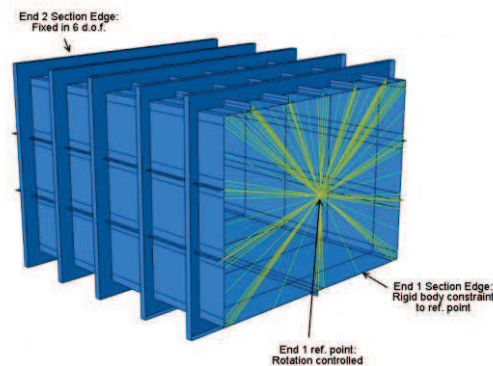


Fig. 4: Test Section Model Boundary Conditions

One end of the section is constrained in all 6-degrees of freedom. The other end is tied to a reference point using rigid body constraints. Rotation is applied at the reference point with all other degrees of freedom unconstrained. This effectively creates the same boundary as at the fixed end but with the plane free to translate bodily. Note that the position of the reference node is arbitrary and does not have to coincide with the neutral axis. The rotation of the rigid body is then controlled in the analysis to cause progressive application of pure bending moment in the mid region, which is ensured because the end bays are shorter and thus less susceptible to interframe buckling than the central bays.

To demonstrate the validity of the test section model for comparison with the physical experiment results, a complete representation of the 4-point bending rig was also developed. This enabled the test section to be loaded in the same manner as followed in the original experiment (Fig. 5b). The model is pinned at the outermost supports and bending moment is imparted in the central section using displacement controlled constraints at the load application points.

### Mesh

All models were meshed using Abaqus S4R quad elements, with S3 triangular elements used where necessary to mesh round complex features such as the frames. S4R is a 4 node doubly curved finite strain element with reduced integration. The default in plane displacement hourglass control within Abaqus is employed. A mesh convergence study was undertaken to indicate the required element size to generate consistent results. A 20mm characteristic element length was found to be sufficient.

### Results

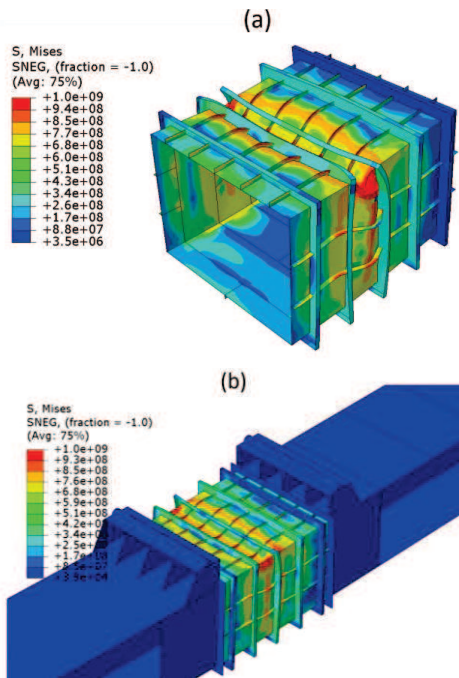


Fig. 5: NLFEM mesh plots for F200 test: (a) specimen model, (b) complete model

The NLFEM bending moment-curvature plots in Fig. 6 generally show relatively poor correlation with the physical test results. The NLFEM predicts lower ultimate strength by about 20% in the F200 and F300 specimens. The F400 specimen results show a much closer correlation, with the NLFEM predicting only a slightly decreased ultimate strength. However, the NLFEM results all show lower initial stiffness. It is possible that this may be caused due to additional support of the upper flange due to the supports in the physical experiment. A more detailed analysis and explanation of this discrepancy is given in Benson et al. (2013).

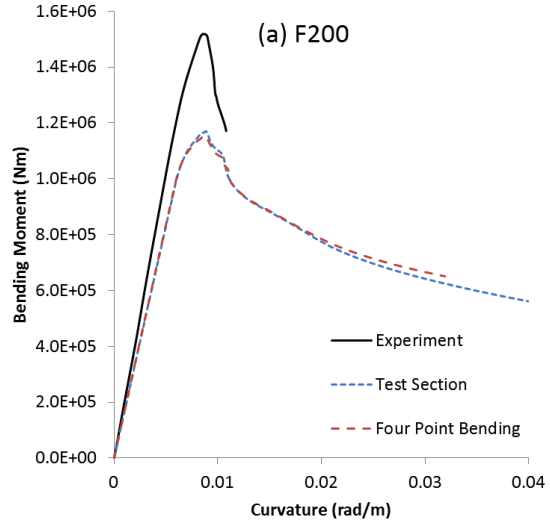


Fig. 6. ????

The quasi static Riks method is also compared to an equivalent nonlinear dynamic-explicit NLFEM analysis to demonstrate the suitability of the quasi-static post collapse characterisation. The small size of the IST box girders means that they are well suited to an efficient analysis without excessive computational effort.

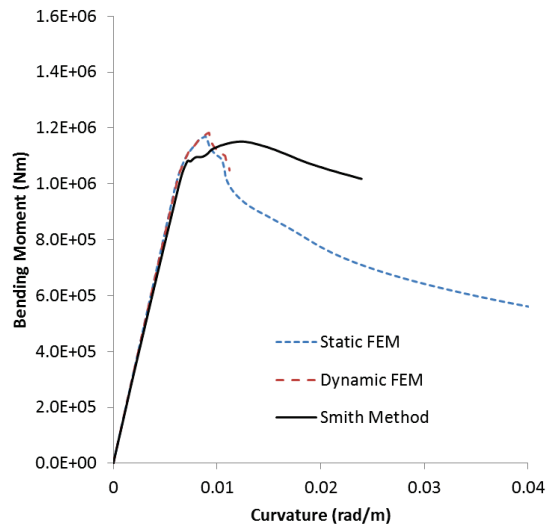


Fig. 7: Comparison of NLFEM solvers with vertical (sag) bending moment

Results are presented in Fig. 7. The static and dynamic approaches produce almost identical behaviour. The findings suggest that the quasi static Riks approach is an acceptable solver method even when handling a highly nonlinear post collapse scenario. The results are so close as to suggest that box girder collapse is essentially quasi-static, even when the peak of the bending moment curve is sharp and the unloading portion of the curve is steep.

### Analysis of Damaged Girders

The latter part of this paper presents progressive collapse analysis of the box girder with damage first sustained from an artificial indenter. The purpose of the analysis is to compare the predictions of damaged box

girder ultimate strength with and without residual stress using dynamic explicit, implicit and static analysis. This section discusses the simulation of indentation damage of the box girder using dynamic explicit analysis. The results focus on the load of the indenter that punches into the box girder with constant velocity and to a depth of 0.3m. The following section presents and discusses the results from subsequent progressive collapse analyses of the damaged structures.

### Simulation Approach

The numerical simulations are undertaken with 3 load steps:

- Step 1: penetration of the indenter into the box girder at 3m/s and to a depth of 0.3m,
- Step 2: retraction of the indenter at 3m/s,
- Step 3: apply incremental bending moment up to and beyond the ultimate capacity

Where Step 3 is completed using the dynamic solver a step time of 1 second was used to increment the applied curvature from zero to the post collapse region.

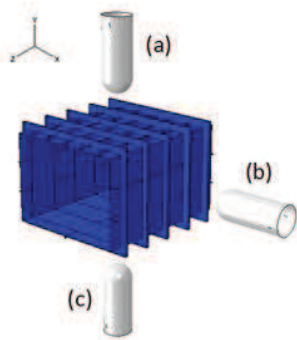


**Fig. 8: Indentation Scenarios (a) Top Indentation, (b) Side Indentation and (c) Bottom Indentation**

The indenter is defined as a rigid body cylinder with a hemisphere tip. The indenter has a size of 0.75m height and 0.35m diameter. The NLFEM analysis used the dynamic explicit analysis capabilities of ABAQUS. Three different indentation scenarios were completed, damaging the bottom, the side and the top flanges of the box. In each case the indenter was targeted at the exact centre of the flange (Fig. 8). The penetration was sufficient to severely rupture the flange around the targeted area. The box boundaries are constrained in all six degrees of freedom for the first two steps. All other initial settings for the NLFEM analysis were the same as for the intact analyses, with superimposed average geometric imperfections.

The indentation of the box girder at top, bottom and side are completed in a separate simulation file before the subsequent bending moment analyses, using the restart capabilities of ABAQUS. This reduced the time cost of the various analyses considerably as multiple bending moment simulations could be completed using a single indentation simulation.

On completion of the indenter analysis steps, the ruptured box girder NLFEM models are further subjected to incremental bending moments to assess their progres-

sive collapse and ultimate strength characteristics. The NLFEM progressive collapse analyses of the damaged box girders are carried out using three approaches, which are now summarised.

The setup is generally as detailed previously, with the boundary conditions modified to the constraints shown in Fig. 4. A full range of curvature combinations are simulated to produce complete interaction curves for comparison with the equivalent intact results. The analysis also allows comparison of several different NLFEM solver approaches. Three distinct setups were followed: an explicit analysis including the residual stresses due to damage; an explicit analysis excluding the residual stresses due to damage; and an implicit analysis also excluding the residual stresses due to damage.

### Results - Top Damage

The interaction plots (Fig. 9) show the significant reduction in ultimate capacity of the top damaged box compared to the intact strength in almost all cases. The reduction is most pronounced in the upper part of the interaction plot, where the box is under sagging bending moment. In this circumstance the damaged region is placed under compressive in plane load. This is predominantly taken by the upper parts of the box sides. Compared to the intact box, the compressive load portion of the cross section is also increased for the same curvature because the neutral axis is lower. These effects combine to cause much earlier buckling in the upper parts of the box, which corresponds to a much lower ultimate strength. The reduction in ultimate strength is less significant in the lower (hog) part of the interaction plot.

The interaction plot also shows considerable differences between the NLFEM analyses where the residual stress due to damage is maintained (dynamic NLFEM with residual stress) and the equivalent analyses undertaken with no residual stresses included (static NLFEM). The simplified progressive collapse results show close correlation to the static NLFEM. Remarkably, under a predominant hogging bending moment the dynamic NLFEM ultimate strength results are greater than for the intact case, although the capacity is still much reduced in the upper quadrants of the interaction plot.

These results suggest that the residual stresses in the structure, which are particularly high in the region adjacent to the ruptured zone, have a significant effect on the ultimate strength of the girder, in this case by increasing the capacity for all combinations of applied curvature. Both the static NLFEM and simplified progressive collapse results do not account for the influence of the residual stresses.

The top damage box girder results from the static approach and the dynamic – zero residual stress approach are compared in Fig. 10. The results reiterate the findings from the intact analyses showing that the two solvers produce almost identical results so long as the initial conditions in the mesh are identical. This also shows conclusively that the differences between the static and dynamic results presented above are due to the residual stresses in the mesh resulting from the impact.

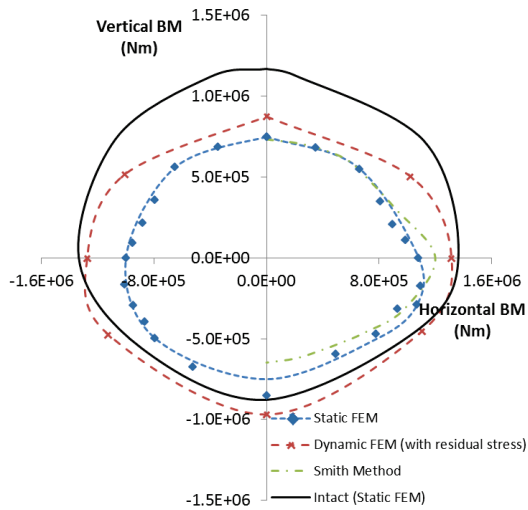


Fig.9: Interaction Diagram for Top Damage

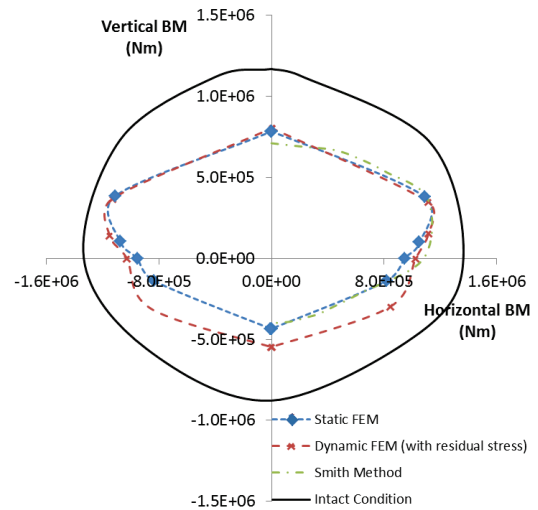


Fig. 11: Interaction Diagram for Bottom Damage

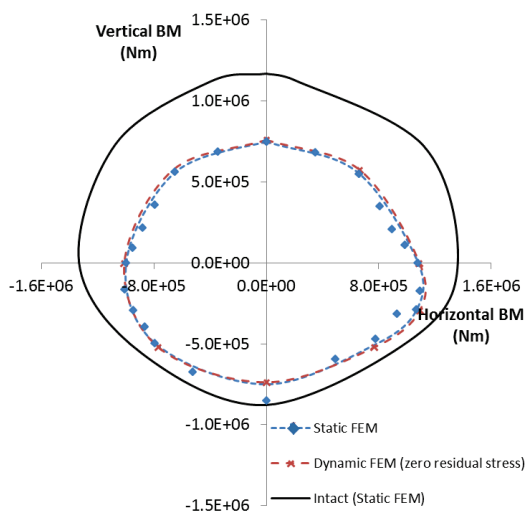


Fig. 10: Comparison of implicit and explicit (zero residual stress) solver methods (Top Damage)

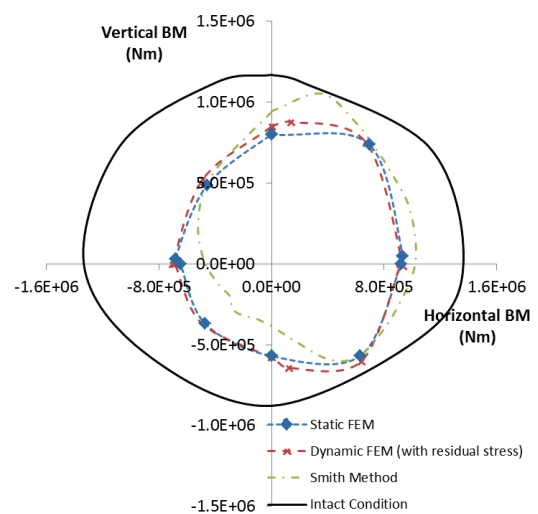


Fig. 12: Interaction Diagram for Side Damage

### Results - Bottom and Side Damage

Interaction plots for the bottom damage scenario are presented in Fig. 11. Interaction plots for the side damage scenario are presented in Fig. 12. In comparison to the differences shown for the top damage case, the plots demonstrates much closer correlation between the static NLFEM, dynamic NLFEM and simplified progressive collapse results. However, the dynamic NLFEM with residual stress results still shows higher ultimate strength than the equivalent zero stress static NLFEM when the box is predominantly under a hogging bending moment, which corresponds to the damage region being placed under compressive load.

The closer correlation between results is likely to be because the top flange, which in this scenario is left intact, is the dominant load bearing region of the structure. Therefore, the influence of the ruptured zone and the associated tensile residual stress field in the bottom flange has less influence on the overall strength of the box under longitudinal bending.

### Conclusions

The strength of three small scale box girder structures have been analysed using several numerical methods under combinations of longitudinal bending moment. The girders have been tested whilst intact and also with three damage scenarios, whereby the girder had been previously subject to an impact simulation which ruptured a large hole in the top, side or bottom flange.

The results have provided numerical verification of the IST box girder experiments [3], and have further elaborated on the reasons why numerical results do not correlate closely with the original experiments. A hypothesis is proposed and validated showing that the friction between the load box and the test section may give rise to an artificial increase in the strength of the box girder. Although this hypothesis is only based on the information of the physical test as published, it provides a reasonable explanation for the discrepancy between numerical and experimental results.

The comparison between static and dynamic NLFEM solvers for the intact box girder has shown that either approach is valid for the purposes of progressive col-



lapse analysis. The assumptions inherent in the static method, which neglects the influence of time dependent mass and damping effects, are acceptable for progressive collapse even when the buckling is essentially a dynamic phenomenon. The results have also demonstrated that the simplified progressive collapse method provides very good results in comparison to the more computationally expensive NLFEM.

However, the damage simulations and the subsequent progressive collapse analyses have shown that the residual stress caused by the impact from a rigid body has a significant influence on the ultimate strength characteristics of a ruptured box girder. Residual stresses are not accounted for in the simplified progressive collapse method or in the static NLFEM analyses as conducted in this study. In the dynamic NLFEM analyses the residual stress, in the form of large tensile zones close to the ruptured zone and lesser compressive stresses elsewhere, have the effect of increasing the box girder strength by up to 10%.

The results presented in this paper have important implications in the development of approximations of rupture and damage in both NLFEM and simplified methods. If rupture is modelled by simply removing structural elements the influence of the residual stresses caused during the initiation of the damage is not accounted for and thus its influence on the overall strength of the girder is neglected. A more rigorous approach to representing the structure adjacent to a ruptured zone may be needed so as to properly account for the significant influence of the stresses within the structure.

## Acknowledgement

This study was performed under an Office of Naval Research grant. The authors would like to thank ONR for their continuing support of this work.

## References

- AbuBakar, A., Dow, R.S., 2010. Simulation of grounding damage using the finite element method, in: International Conference of Collision and Grounding of Ships.
- AbuBakar, A., Dow, R.S., 2013. Simulation of ship grounding damage using the finite element method. *Int. J. Solids Struct.* 50, 623–636.
- AbuBakar, A., Dow, R.S., Tigkas, I.G., Samuelides, M.S., Spyrou, K.J., 2010. Investigation of an actual collision incident between a tanker and a bulk carrier, in: 11th International Symposium on Practical Design of Ships and Other Floating Structures. Presented at the PRADS 2010, Rio de Janeiro, Brazil, pp. 201–211.
- Alsos, H.S., Hopperstad, O.S., Törnqvist, R., Amdahl, J., 2008. Analytical and numerical analysis of sheet metal instability using a stress based criterion. *Int. J. Solids Struct.* 45, 2042–2055.
- Amlashi, H.K.K., Moan, T., 2009. Ultimate strength analysis of a bulk carrier hull girder under alternate hold loading condition, Part 2: Stress distribution in

- the double bottom and simplified approaches. *Mar. Struct.* 22, 522–544.
- Benson, S., AbuBakar, A., Dow, R.S., 2013. A comparison of computational methods to predict the progressive collapse behaviour of a damaged box girder. *Eng. Struct.* 48, 266–280.
- Benson, S., Downes, J., Dow, R.S., In press. Compartment level progressive collapse analysis of lightweight ship structures. *Mar. Struct.*
- Ehlers, S., 2010. Strain and stress relation until fracture for finite element simulations of a thin circular plate. *Thin-Walled Struct.* 48, 1–8.
- Ehlers, S., Benson, S., Misirlis, K., 2013. Ultimate strength of an intact and damaged LNG vessel subjected to sub-zero temperature. Presented at the International Conference on Collision and Grounding of Ships, In press.
- Ehlers, S., Tabri, K., 2012. A combined numerical and semi-analytical collision damage assessment procedure. *Mar. Struct.* 28, 101–119.
- Gordo, J.M., Guedes Soares, C., 2009. Tests on ultimate strength of hull box girders made of high tensile steel. *Mar. Struct.* 22, 770–790.
- Gordo, J.M., Guedes Soares, C., 2011. Compressive tests on stiffened panels of intermediate slenderness. *Thin-Walled Struct.* 49, 782–794.
- Jie, M., Cheng, C.H., Chan, L.C., Chow, C.L., 2009. Forming limit diagrams of strain-rate-dependent sheet metals. *Int. J. Mech. Sci.* 51, 269–275.
- Keeler, S.P., Backofen, W.A., 1964. Plastic instability and fracture in sheets stretched over rigid punches. *Asm Trans. Q.* 56, 25–48.
- Kutt, L.M., Piaszczyk, C.M., Chen, Y.-K., Liu, D., 1985. Evaluation of the longitudinal ultimate strength of various ship hull configurations. *Trans. Soc. Nav. Arch. Mar. Eng.* 93, 33–53.
- Paik, J.K., Mansour, A., 1995. A Simple Formulation for Predicting the Ultimate Strength of Ships. *J. Mar. Sci. Technol.* 1, 52–62.
- Qi, E., Cui, W., Wan, Z., 2005. Comparative study of ultimate hull girder strength of large double hull tankers. *Mar. Struct.* 18, 227–249.
- Sedlacek, G., Müller, C., 2001. High Strength Steels in Steel Construction, in: Niobium: Science & Technology. Presented at the International Symposium Niobium 2001, TMS: The Minerals, Metals & Materials Society, Orlando, Florida.
- Smith, C.S., 1977. Influence of local compressive failure on ultimate longitudinal strength of a ship's hull, in: Practical Design of Ships and Other Floating Structures. Presented at the PRADS77, Tokyo, Japan.
- Wevers, L.J., Vredeveldt, A.W., 1999. Full Scale Ship Collision Experiments 1998: Test of New Type Ship Side Structure, Royal Schelde, the Netherlands. TNO.